

Original Article

Control of Floating Object Directions on Rip Current at Beaches by Using Deflectors

Reda M. A. Hassan¹, Ibrahim M. A.², Mohb M. Iskander³, Mostafa M. A.⁴

¹*Oceanography Department Head, Coastal Research Institute, National Water Research Center, Alexandria, Egypt*

^{2,4}*Coastal Research Institute, National Water Research Center, Alexandria, Egypt.*

³*Hydrodynamic Department Head, Coastal Research Institute, National Water Research Center, Alexandria, Egypt*

Corresponding Author : Doctor_Reda2010@yahoo.com

Received: 01 September 2022

Revised: 20 December 2022

Accepted: 18 January 2023

Published: 24 January 2023

Abstract - This paper introduces an innovative deflector system to reduce the threats of rip currents. This research aims to assess the proposed tool to deflect the floating subjects caught by rip currents, study the effect of deflector angles on the values and directions of the rip current velocities, and investigate the effect of the deflector distances from the shoreline on rip currents. To achieve the study objectives, experimental works, field measurements, numerical works using the Mike21 model, and mathematical formula derivation of different parameters were carried out. The proposed deflector systems were modeled with different shapes and materials. The experiments were executed first without placing the proposed deflectors as a reference case (A). Then three different types of the proposed deflectors were checked with different water depths (5, 7.5, 10, and 15 cm), different wave frequencies (15, 20, 25, 30, 35, and 40 min⁻¹), and different distances (95, 105, and 125 cm) for the deflector seaward from the shoreline were examined. The rip current velocities have inversed in relation to the distance of the deflector from the shoreline. It is concluded that the deflectors can direct the floating bodies and materials at an angle away from the center of rip currents. This study concludes that the use of deflectors can mitigate drowning effects and increase the preservation of lives. Finally, it is recommended for decision-makers that the proposed deflector should be checked and modified using prototypes in the field conditions; after that, it can be used as a new tool to deflect rip currents to save lives.

Keywords - Rip current, Drowning, Behavior of floating body, Rip current direction, Deflector.

1. Introduction

The phenomenon of a rip current is one of the causes of many drowning cases on all the world's beaches. This phenomenon consists of forming a water channel in the surf zone at the shore. As a result of the feeder streams parallel to the shore, these feeders form a bed water channel perpendicular to the shore. The return current through this channel increases the water speed and increases the bed erosion of the channel. The velocity of the current through those channels may reach speeds that no Olympic champion in swimming can resist. Losses due to drowning from currents, particularly rip currents, are the most important hazard on global beaches, Reda M., Shaimaa E., 2019, [18]. Dalrymple, 1978 [5] studied rip currents and their causes; the study showed that rip currents move large amounts of sand, so the rip channel is similar to a little river. Generally, the narrower the surf zone is, the stronger the rip current will be. The three main types of rip currents are hydrodynamically and bathymetrically. Structurally controlled rips, Gallop et al., 2016, [4], also Mac Mahan et al., 2011, [15] studied the rip currents based on field observations; the study showed that the rip current has three components; the feeder current, which is formed by the moving of water body along and parallel to the shoreline, the neck of rip that is continued and maintained by feeder currents from both side or only one

side, and the head of the rip in which the velocities decrease and the flow diffuses. Taha. S., 2016, [21] studied the hydraulic analysis of the circulations and rip currents at Baltim detached breakwaters localities using field data and the Mike 21-FM flow model; the study showed that the current velocity ranges from 0.20 m/s to more than 0.70 m/s in the surf zone. The currents over one m/s are found in many coastal areas of the world Hedges, T.S., (1987). Hedges, T.S., 1987, [23] studied the complex interactions between waves and currents. The study presented a good understanding of how waves behave in the presence of currents. The study discussed a train of regular waves (wavelength L, height H) traveling on a steady, horizontally, and vertically uniform current. The study concluded that currents have significant effects on wave speed and direction. Haller, M. C., 1999, [10] studied the rip current dynamics and nearshore circulation using a physical model consisting of a longshore bar on a planar beach with two rip channels. The experiments demonstrated the presence of low-frequency rip current oscillation and also the presence of two circulation systems. Flow characteristics in the rip neck were narrow, offshore directed, and exhibited the strongest flow velocities. The rip current formed a closed circulation cell in conjunction with the onshore water mass transport in the breaker zone. In general, the rip velocity values were more



than 0.2 m/s and may reach 3.0 m/s. Brewster et al., 2019 [2] and Gensini V.A. et al., 2009 [8] showed that rip currents were the maximum hazard to swimmers on surf beaches in the USA. Central Agency for Public Mobilization and Statistics Egypt CAPMAS, 2018, [3] showed that drowning accidents and immersion in water unintentionally was about 7% of totally different accidents in Egypt; around 1054 male and 220 female were drowned via drowning accidents in 2017 only. Egyptian Northern coasts are classified as dissipative beaches which create medium-risk rip currents, especially during the spring and summer seasons, Iskander et al., 2021, [12] also Winter, G. 2012, [25], Morang et al., 1993, [16] studied the geologic, geomorphic history of coasts using field data collection and observation. Svendsen et al., 2003, [19], Tae-Myoung, et al., 1996, [26]; Vriend et al., 1987, [24]; Haas, K. A et al., 2003, [9] studied quasi-three-dimensional modeling of the rip current system, and all the studies recognized the rip currents on the different coasts; also, Herrington, 2012, [11] studied the fundamentals of nearshore rip currents, Elmooty, and Taha, 2012-B, [7] studied the rip currents using the Mike 21-FM flow model. The study identified the rip currents on the northern coast of Egypt. Bader and Shata, 2002, [1] studied the effect of Baltim detached breakwaters on grain size variations and littoral sand drift.

The study showed that rip currents played a significant role in carrying sediments offshore through the breaker zone. Many studies and inventions have been carried out and submitted to practical applications to control rip currents. Thomas, 2004, [22] introduced patent no. US6738992B2 in the United States with the title "Method and apparatus for controlling breakpoints and reducing rip currents in wave pools" The main idea of the invention was to provide a grates section to a portion of the floor or the beach; the grates will allow water to pass into a cavity, which eliminates backflows and consequently, rip currents will be averted. Kim et al., 2012 [13] introduced patent no. KR20120069253A in South Korea, with the title "Disaster prevention and alarm system for rip current". The invention was a flow prediction deflector, using a large number of velocity buoys installed at sea level in the area where the rip current was expected. Lee, 2013 [14] introduced patent No. KR101221688B1 in South Korea, with the title "Rip Current Detection Float". The invention consisted of a buoy designed to move along the flow of rip currents to determine the rip current velocity within the wave area. Earl Sinchuk et al., 2013, [6] introduced patent No. US 2013/0181842 A1 titled "Rip Current Sensor and Warning System with Anchor". The sensor was easily installed to detect the rip current close to the shore or other swimming areas to warn people in the water and on the shore of the presence of a rip current. N. Wallace and Quarry, 2015, [17] the US introduced patent No. 9,180,937 B2 for water safety equipment used in marine environments. The innovative concept was that a safe marine buoy is moored in the surf zone to indicate the presence and

direction of the rip currents and provide a platform near those who require assistance. Hassan, R.M. and Hassan, S.E.T., 2019, [18] solved the rip current problems by deploying innovative warning floating self-lighting units along the rip current path.

2. Objectives

The present study discusses the possibility of using a new innovative deflector as a new tool to control rip currents. The objectives of this research are:

- The assessment of the efficiency of the proposed deflectors to deflect the floating subjects caught by rip currents and the rip current behavior,
- Studying the effect of deflector angles on the values and directions of the rip current velocities,
- Studying the effect of the deflector distances from the shoreline on rip currents.

3. Materials and Methods

3.1. Experimental Settings and Numerical works

The experimental works were performed at the physical model lab of Abu Quir research station, Coastal Research Institute (CoRI), National Water Research Center (NWRC), Alexandria, Egypt. The physical model lab has a wide wave flume with dimensions (40.0×1.2×1.2 m). The flume has flab-type wave generation and passive-type wave absorption systems. Experimental Works can be concluded in these points: 1-Flume preparation, 2-Design of rip current morphology, 3-Adjusting of cameras, 4-Calibration of wave height measuring devices, 5-Preparation of proposed deflectors, 6-Adjusting of flume gate and absorbers, 7-Choosing of water depths 5,7.5,10, and 15 cm, 8- Choosing of frequencies 20,25,30,35, and 40 r.p.m, and significant wave heights, 9- Preparation of proposed floating objects, 10- The setting of reference case (A) without deflectors, 11- Choosing the three experimental cases (B, C, and D) at different distances (95.0, 105.0, and 125.0 cm). The shoreline and the bed morphology were designed to form an ideal fixed rip current type. Figures (1-A, B, C, and D) show the general perspective of bed morphology and different cases at the flume. The bed morphology was prepared to create a fixed bed for the rip current generation. Different shapes and materials also represented the deflector units. The deflector models were placed in the path of the generated rip currents at different distances from the shoreline in the flume. As a reference case (A), 20 experimental runs were conducted without placing the proposed deflectors. The experiments were executed as mentioned before with different water depths (5.0,7.5,10.0, and 15.0 cm) and different frequencies (20.0,25.0,30.0,35.0, and 40.0 min⁻¹) as well as different forms of the deflectors using concrete and perforated plastic materials. The concrete type has two forms: one curved towards the beach and the second towards the sea; the perforated plastic type has two forms, one curved towards the beach and the second towards the seaside.

A wave gauge was installed upstream of the generated morphology for measuring and calculating the different properties of the generated waves (wavelength λ , wave period T, and significant wave height Hs). Then, three groups of experimental cases (B, C, and D) with the same conditions above were conducted by placing the deflector at three

different distances (95.0 cm, 105.0 cm, and 125.0 cm) measured seaward from the shoreline. Data gathering of the traveled distances by the floating objects to come back to the shoreline at a certain angle (θ) in the direction of the sea and the Return time of floating objects at a certain angle (θ) in the direction of the sea.

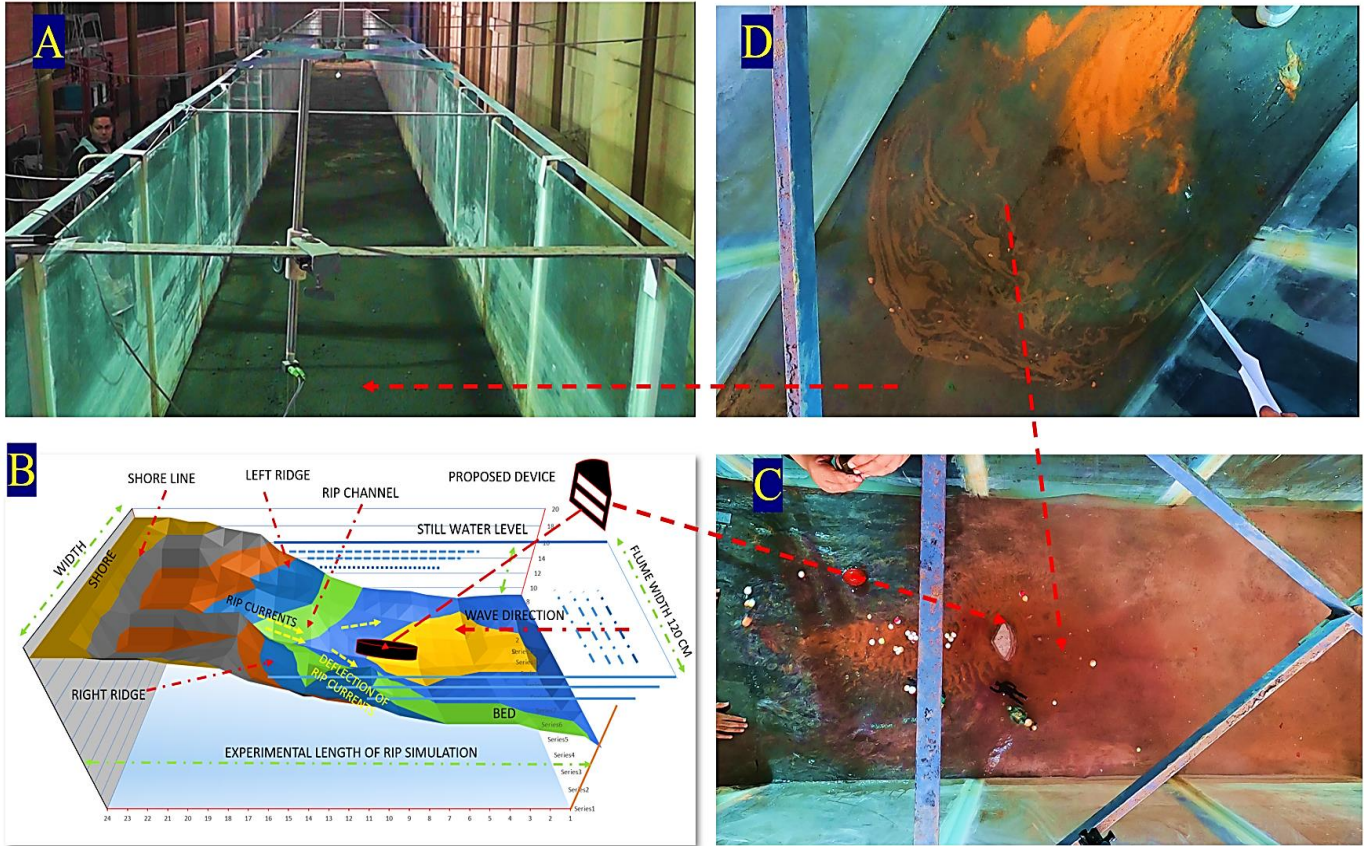


Fig. 1-A, B, C, and D The general perspective of the physical wave flume, the bed morphology used to simulate the rip currents, the fluorescent sand in orange color showing the rip current surface plume, the different floating materials and the proposed concrete deflector within the physical flume experimental works.

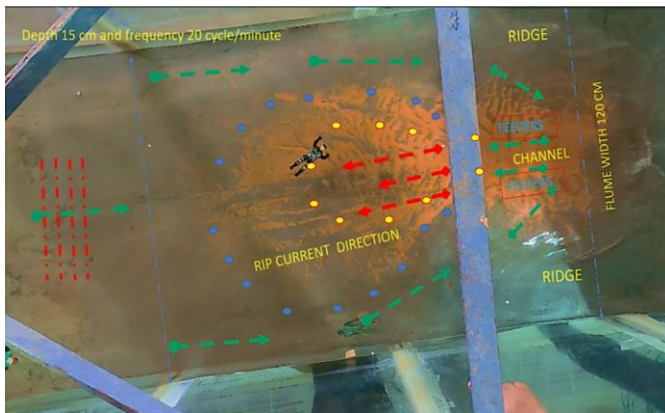


Fig. 2 Shows the projected view of the experimental case (A) without deflectors; the rib current feeders were explained with green color arrows, the rip current boundaries were explained with dots of blue and yellow colors, and the waves and streamlines were explained with red color arrows.

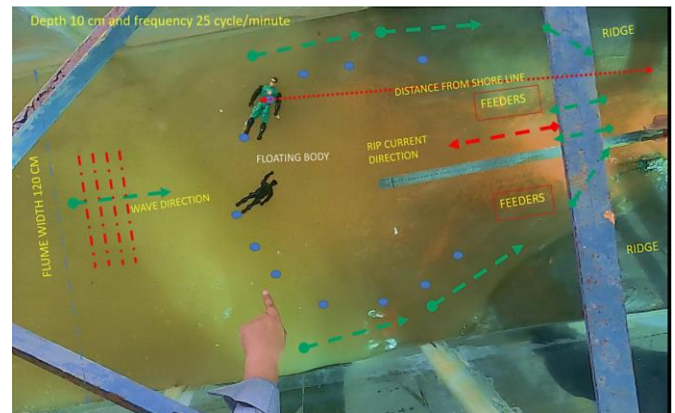


Fig. 3 Shows the floating objects in green and black colors and the projected view of the experimental case (A) without deflectors, the rib current feeders were explained with green color arrows, and the rip current boundaries were explained with dots of blue and yellow colors, and the waves and streamlines were explained with red color arrows.

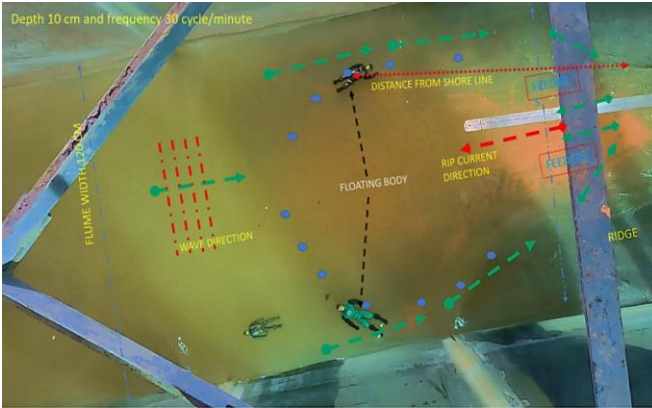


Fig. 4 Shows the behavior of floating bodies in the surface plume of rip currents and the projected view of the experimental case (A) without deflectors; the rib current feeders were explained with green color arrows. The rip current boundaries were explained with dots of blue and yellow colors, and the waves and streamlines were explained with red color arrows.

Figure (2) shows the projected view of the experimental case (A) without deflectors. The rib current feeders were explained with green color arrows, the rip current boundaries were explained with dots of blue and yellow colors, and the waves and streamlines were explained with red color arrows. Figure (3) shows the floating objects in green and black colors and the projected view of the experimental case (A) without deflectors, the rib current feeders explained with green color arrows. The rip current boundaries are explained with dots of blue and yellow colors, and the waves and streamlines are explained with red arrows. Figure (4) shows the behavior of floating bodies in the surface plume of rip currents and the projected view of the experimental case (A) without deflectors, the rib current feeders were explained with green color arrows, and the rip current boundaries were explained with dots of blue and yellow colors, and the waves and streamlines were explained with red color arrows. To achieve the goals of this research, a comparison between experimental and numerical works should be done, so field measurements were carried out using collected data from Coastal Research Institute (CORI) and Egyptian Authority for Shore Protection (SPA). The chosen area includes breakwaters at the Egyptian north coastal zone between longitudes 29° 43' E and 29° 42' E and latitude 31° 6' N. Applying (MIKE21) using full data of waves, water depths, and bed characteristics at the study area. In the study area, the wave direction was chosen Northwest, according to the real data of the dominant direction of waves near the shoreline. A better representation of the bathymetry and the model simulation was optimized satisfactorily.

3.2. Description of proposed Deflector Elements and their Mechanism

This study proposed the new deflector, which consists of four main parts; will be referring to them as shown in Figures (5 and 6): - (1) - Front part(1-a), (2) - Rear part(1-b), (3) - Lower part(1-c), and (4) - Upper part(1-d). The sides of the

deflector, rear part, and front part have grooves, which deflect and redirect the stream lines' directions of the rip currents. For an observer at the shore as a stationary reference to the position of the proposed deflector, the front part of the deflector (1-a) directs the rip current away from the sea directly to the right and left sides of the deflector. The horizontal angle of inclination of the front part (1-a) is controlled by the angle (θ), this angle is less than (180) degrees and greater than (zero) degrees, and it is defined in this study as the angle between the two sides of the deflector in the front part (1-a). The back part of the deflector (1-b) guides the waves coming from the sea direction to shore. There are grooves within this part to direct the waves in a direction nearly parallel to the shore and tangential to the curved part(1-b). The tangential wave component of the subsequent waves with lag time equals wave period (T) confronts the directed rip current coming from the front part (1-a). As a result of this confrontation, a new resultant rip current streamline is created with a value and direction that depends on the speed and direction of both the directed currents and the tangential wave component of the subsequent waves. This net streamline creates a natural water obstruction, nearly parallel to the shore, that prevents users from being drawn toward the sea.

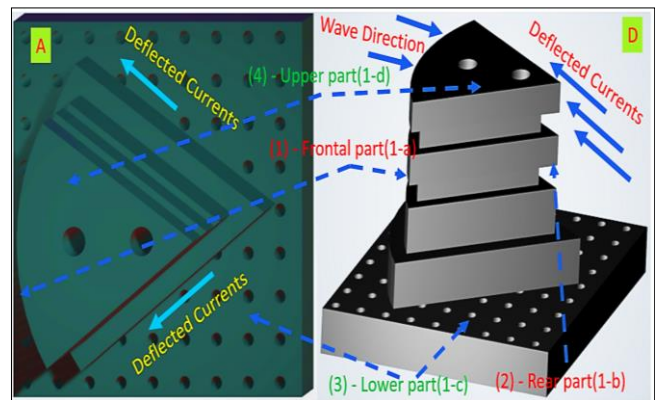


Fig. 5 The perspective and the top view of the proposed deflector with its main elements showing the frontal part, rear part, upper part, and lower part, in addition to the side grooves, vertical holes, and the direction of deflected currents

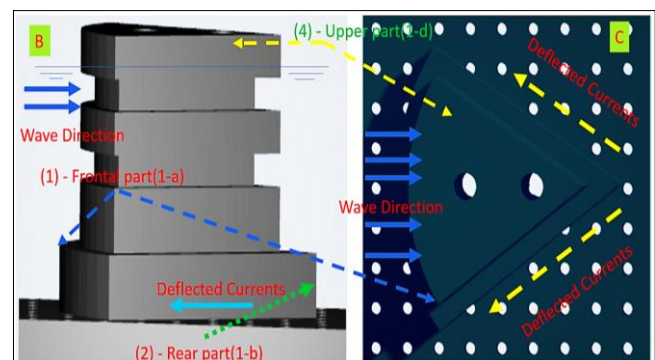


Fig. 6 The side view and the plan view of the deflector and its main elements showing the direction of waves, water level, side grooves, vertical holes, and the direction of deflected currents

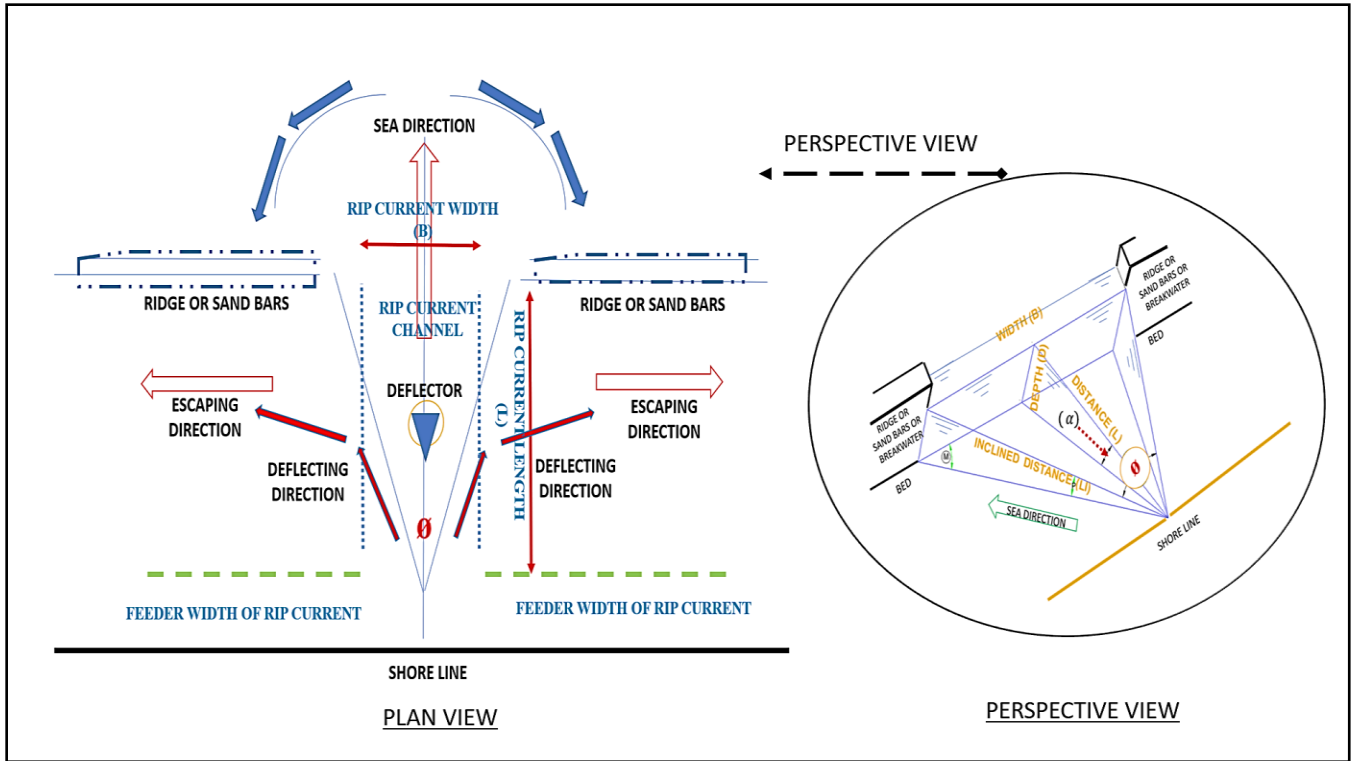


Fig. 7 The plan and perspective view showing the different rip current parameters like the surface plume, ridges or sand bars, formed bed channel by rib currents, the width of rib current, the direction of escaping for swimmers, details of the proposed deflector locations and its inclination angle, also showing the relation among the deflector-designed angles, water depths and distances to shore.

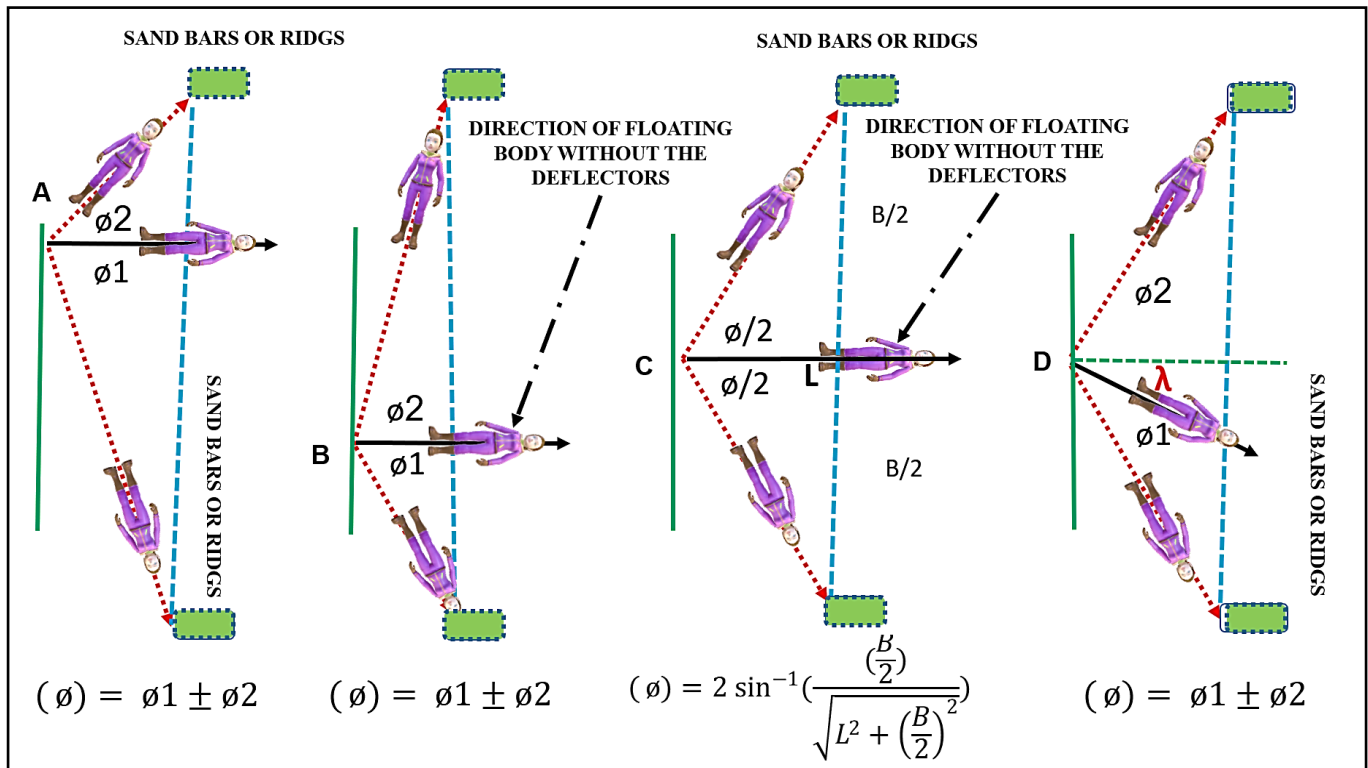


Fig. 8 The behavior of floating subjects according to the different designed angles of the proposed deflector at different points and directions, the plan view shows the proposed four different scenarios of rip current locations and directions at points A, B, C, and D. The ridges or sand bars were explained in green color blocks, shorelines in green color lines, and distances between sand bars in blue color dotted lines, also the relation between the deflector-designed angles, and distances from deflectors to the shoreline was explained in simple equations.

The deflector is installed through the lower part of the deflector (c-1) using an appropriate method, where slots are made through which. The deflector can be installed at the bottom of the water rip channel using plastic or stainless screws and using plastic or steel flanges. The bottom slope is leveled at the bottom of the deflector using a rib-wrap size appropriate to the deflector's weight and the bottom's nature.

3.3. Getting the Designed Angle of the Deflector

Rip current can be detected using different methods like colored soluble materials like dye. It can also be detected visually by observers at elevated places like shore guideposts and flying drowns. Rip currents usually have a perpendicular direction to the shore but sometimes have an inclined angle to the shore direction, depending on the nature of the shore, the nature of the currents, and the morphology of the bottom around the rip currents. The threats of rip currents come from this angle with the shore because the currents draw any swimmer or beach user directly to the offshore direction.

So, controlling rip currents comes from the design of the horizontal inclination angle of a deflector (θ), which can control the rip current at any angle depending on the shore's nature, the current's nature, and the morphology of the bottom around the rip current. Figures (7) and (8) demonstrate the mathematical parameters at sand bars and ridges to get the horizontal designed angle of proposed deflector sides to deflect rip currents, where: (L) is the horizontal distance from the shoreline to sand bars and ridges perpendicular to it at still water level conditions, (Li) is the horizontal inclined distance from the shoreline to edges of sand bars or ridges at sea water level, (D) is the water depth at sand bars or ridges, (B) is the width of rip current in between sand bars, (Ls) is the inclined distance from the shoreline to sea bed level at sand bars, (Lg) is the inclined distance from the shoreline to edges of sand bars at sea bed level, (θ) is the horizontal designed angle of the proposed deflector of two sides, ($\theta/2$) is the inclination angle of the proposed deflector on one side from the perpendicular line to shore (L). The inclined distance (Ls) can be obtained from equation (1) as follow:

$$Ls^2 = L^2 + D^2 \tag{1}$$

also, (Lg) the inclined distance from the shoreline to the edges of sand bars at sea bed level and (Li) the horizontal inclined distance from the shoreline to edges of sand bars at seawater level can be obtained from equations (2), (3), and (4).

$$Lg^2 = Ls^2 + \left(\frac{B}{2}\right)^2 \tag{2}$$

$$Lg^2 = Li^2 + D^2 \tag{3}$$

$$Li^2 = Lg^2 - D^2 \tag{4}$$

The angle of inclination of the proposed deflector on one side from the horizontal line (L) to the right or left ($\theta/2$) can be gotten from equation (6) by substituting from equation (5) by (Li).

$$Li^2 = Ls^2 + \left(\frac{B}{2}\right)^2 - D^2 \tag{5}$$

$$\sin \theta/2 = \left(\frac{B}{2}\right)/Li \tag{6}$$

also, by substituting in equation (7) by (Ls),

$$\sin \theta/2 = \left(\frac{B}{2}\right)/\sqrt{(Ls^2 + \left(\frac{B}{2}\right)^2 - D^2)} \tag{7}$$

Using the derived equation (10) to obtain the horizontal designed angle of proposed deflector sides to deflect rip currents (θ) concerning (B) the width of rip current in between sand bars and (Ls) the inclined distance from the shoreline to sea bed level at sand bars, after rearranging equations (8) and (9).

$$(\theta) = 2 \sin^{-1}\left(\frac{B}{2}\right)/\sqrt{(Ls^2 + \left(\frac{B}{2}\right)^2 - D^2)} \tag{8}$$

Where: $Ls^2 = L^2 + D^2$,

$$(\theta) = 2 \sin^{-1}\left(\frac{B}{2}\right)/\sqrt{(L^2 + D^2 + \left(\frac{B}{2}\right)^2 - D^2)} \tag{9}$$

$$(\theta) = 2 \sin^{-1}\left(\frac{\left(\frac{B}{2}\right)}{\sqrt{L^2 + \left(\frac{B}{2}\right)^2}}\right) \tag{10}$$

The horizontal designed angle of the proposed deflector sides to deflect rip currents (θ) can be calculated if the rip currents are not perpendicular to the shoreline or are not in the middle between sand bars as follows:

$$(\theta) = \theta1 \pm \theta2 \tag{11}$$

To get the deflector arch length (x), it can be calculated from the mathematical relations of the circle, which include the angle θ , where:

$$(x/ 2\pi) = (\theta/360), \text{ then } x = \frac{(\theta Ri\pi)}{180} \tag{12}$$

Where: - (Ri) is the radius of the arch (x), as shown in table (1). where: $\theta1$ is the horizontal designed angle of the proposed deflector's right side to deflect rip currents and is measured from the rip current direction line. $\theta2$ is the horizontal designed angle of the proposed deflector's left side to deflect rip currents and is measured from the perpendicular line onshore to the rip current direction line. Angle $\theta1$ and $\theta2$ can be measured using any available leveling device. Angle θ is greater than zero and less than 180 degrees: ($\theta = 180 - 2 \beta$), where β is greater than or equal to zero and less than or equal to 90, ($0 \leq \beta \leq 90$).

Table 1. shows the calculated values of deflector dimensions, arch length (X), angle (θ) from 0.00 to 180.00 degrees, and radius (Ri) from 1.00 m to 4.00 m as an example of dimensions of deflectors

Deflector Angle	Deflector Radius	Arch L. (m)	Defl. Ang.	Deflect or R.	Arch L. (m)	Defl. Ang.	Deflect or R.	Arch L. (m)	Defl. Ang.	Defl. Radu.	Arch L. (m)
θ degree	R1 (m)	X1 (m)	θ deg.	R2 (m)	X 2(m)	θ deg.	R 3(m)	X3	θ deg.	R4 (m)	X 4(m)
10	1.00	0.17	10	2.00	0.35	10	3.00	0.52	10	4.00	0.70
20	1.00	0.35	20	2.00	0.70	20	3.00	1.05	20	4.00	1.40
30	1.00	0.52	30	2.00	1.05	30	3.00	1.57	30	4.00	2.09
40	1.00	0.70	40	2.00	1.40	40	3.00	2.09	40	4.00	2.79
50	1.00	0.87	50	2.00	1.74	50	3.00	2.62	50	4.00	3.49
60	1.00	1.05	60	2.00	2.09	60	3.00	3.14	60	4.00	4.19
70	1.00	1.22	70	2.00	2.44	70	3.00	3.66	70	4.00	4.88
80	1.00	1.40	80	2.00	2.79	80	3.00	4.19	80	4.00	5.58
90	1.00	1.57	90	2.00	3.14	90	3.00	4.71	90	4.00	6.28
100	1.00	1.74	100	2.00	3.49	100	3.00	5.23	100	4.00	6.98
110	1.00	1.92	110	2.00	3.84	110	3.00	5.76	110	4.00	7.68
120	1.00	2.09	120	2.00	4.19	120	3.00	6.28	120	4.00	8.37
130	1.00	2.27	130	2.00	4.54	130	3.00	6.80	130	4.00	9.07
140	1.00	2.44	140	2.00	4.88	140	3.00	7.33	140	4.00	9.77
150	1.00	2.62	150	2.00	5.23	150	3.00	7.85	150	4.00	10.47
160	1.00	2.79	160	2.00	5.58	160	3.00	8.37	160	4.00	11.16
170	1.00	2.97	170	2.00	5.93	170	3.00	8.90	170	4.00	11.86
180	1.00	3.14	180	2.00	6.28	180	3.00	9.42	180	4.00	12.56

Table 2. The values of measured velocities for different locations of the proposed deflector distances were 0.00 m for reference case A, 95.00 m for case B, 105.00 m for case C, and 125.00 m for case D. The significant wave heights were measured and calculated using measuring devices of wave height according to the frequencies from 20 cycle/min. to 40 cycle/min. The distances were measured in centimeters and time in seconds.

Measured Distance of Deflector from Shore	Frequency	Measured Rip current Length	Measured Time to Pass Rip Neck	Measured Velocity of Rip Current
Distance X(cm) 0.0 cm	cycle/min	L1(cm)	T1(sec)	V1(cm/sec)
Free Case A	20	91.00	9.00	10.11
	25	111.00	14.00	7.90
	30	118.64	19.00	6.24
	35	135.08	26.00	5.20
	40	142.10	37.00	3.83
Average		119.56	21.00	6.66
Distance X(cm) 95 cm	Frequency	L1	T1	V1
Case B with Deflector	20	73.00	6.00	12.17
	25	97.00	10.00	9.70
	30	95.00	8.00	11.88
	35	80.78	11.00	7.34
	40	105.00	10.00	10.50
Average		90.16	9.00	10.32
Distance X(cm) 105 cm	Frequency	L1	T1	V1
Case C with Deflector	20	81.68	6.00	13.61
	25	105.00	10.00	10.50
	30	82.25	10.00	8.23
	35	66.19	9.00	7.35
	40	105.00	13.00	8.08
Average		88.02	9.60	9.55
Distance X(cm) 125 cm	Frequency	L1	T1	V1
Case D with Deflector	20	89.50	8.00	11.19
	25	81.47	9.00	9.05
	30	86.83	12.00	7.24
	35	82.12	19.00	4.32
	40	125.00	20.00	6.25
Average		92.98	13.60	7.61

Table 3. The different percentage values of deflection, due to the presence of deflectors The values of the measured rip current velocities for different locations of the proposed deflector, distances were 0.00 m for reference case A, 95.00 m for case B, 105.00 m for case C, and 125.00 m for case D, the significant wave heights were measured and calculated using measuring devices of wave height according to the frequencies from 20 cycle/min. to 40 cycle/min. The distances were measured in centimeters and time in seconds. It shows the calculated % values of deflected current angles; the angle (θ) was chosen from 0.00 to 90.00 degrees.

Cases	Measured Rip Current (cm/sec)	Frequency	Rip Current Components for Deflector angle 60		Deflector Angle 60		Deflector Angle 45		Deflector Angle 30		Incident Angles
	Um		Y com.	X com.	Deflector Angle	% Def. of Rip curr.	Deflector Angle	% Def. of Rip curr.	Deflector Angle	% Def. of Rip curr.	
Case A - Free	11.20	15	11.20	0.00	No Deflector	0	No Deflector	0	No Deflector	0	90
	10.11	20	10.11	0.00	No Deflector	0	No Deflector	0	No Deflector	0	90
	7.90	25	7.90	0.00	No Deflector	0	No Deflector	0	No Deflector	0	90
	6.24	30	6.24	0.00	No Deflector	0	No Deflector	0	No Deflector	0	90
	5.20	35	5.20	0.00	No Deflector	0	No Deflector	0	No Deflector	0	90
	3.83	40	3.83	0.00	No Deflector	0	No Deflector	0	No Deflector	0	90
Case B - X95cm	14.20	15	7.10	12.30	60	50	45.00	29.29	30.00	13.40	30
	12.17	20	6.08	10.54	60	50	45.00	29.29	30.00	13.40	30
	9.70	25	4.85	8.40	60	50	45.00	29.29	30.00	13.40	30
	11.88	30	5.94	10.28	60	50	45.00	29.29	30.00	13.40	30
	7.34	35	3.67	6.36	60	50	45.00	29.29	30.00	13.40	30
	10.50	40	5.25	9.09	60	50	45.00	29.29	30.00	13.40	30
Case C - X105cm	13.90	15	6.95	12.04	60	50	45.00	29.29	30.00	13.40	30
	13.61	20	6.81	11.79	60	50	45.00	29.29	30.00	13.40	30
	10.50	25	5.25	9.09	60	50	45.00	29.29	30.00	13.40	30
	8.23	30	4.11	7.12	60	50	45.00	29.29	30.00	13.40	30
	7.35	35	3.68	6.37	60	50	45.00	29.29	30.00	13.40	30
	8.08	40	4.04	6.99	60	50	45.00	29.29	30.00	13.40	30
Case D - X125cm	12.00	15	6.00	10.39	60	50	45.00	29.29	30.00	13.40	30
	11.19	20	5.59	9.69	60	50	45.00	29.29	30.00	13.40	30
	9.05	25	4.53	7.84	60	50	45.00	29.29	30.00	13.40	30
	7.24	30	3.62	6.27	60	50	45.00	29.29	30.00	13.40	30
	4.32	35	2.16	3.74	60	50	45.00	29.29	30.00	13.40	30
	6.25	40	3.13	5.41	60	50	45.00	29.29	30.00	13.40	30

3.4. The Effects of Deflectors on the Combinations of Waves and Rip Currents

Using small Foam spheres and plastic models as floating subjects to demonstrate the behaviors of floating bodies or swimmers caught in rip currents, in addition to tiny circular-colored papers, fluorescent sand tracers, and colored dye solution (potassium permanganate and food colors). More than video cameras were installed to observe time and the traveled distances by floating subjects. The different

distances, time intervals, and velocities of the rip currents were measured and calculated for different cases, with and without deflectors (by using the difference in distances and time intervals from video frames).

In addition, the directions of the rip currents were measured and calculated for different cases, with and without deflectors, by using the inclination of floating objects. The inclined angles are measured in the north direction from zero

to 90 degrees clockwise or anticlockwise. The data were measured and tabulated in table (2) for reference case (A). The three experimental cases (B, C, and D), in which (d1) is the traveled distance, (t1) is the elapsed time, and (d2) is the subsequently traveled distance during the elapsed time (t2).

In case (A) without deflector angle (ϕ) equals (0), and the current velocity (U_0) equals 11.20864815, 9.963242797, 8.717837447, 7.472432098, 6.227026748, and 4.981621398 cm/sec, (for angle nearly equals zero, in radians), and time periods 15, 20, 25, 30, 35, and 40 seconds, respectively.

As shown in table (3), measured rip current velocities using the time of floating subjects ($T_{1,2}$) in the path of the rip current, and the traveled distances by the floating subjects from the shoreline ($L_{1,2}$) are calculated by using the following mathematical relations,

$$(\Delta T) = ((T_2) - (T_1)), \text{ and}$$

$$(\Delta L) = ((L_2) - (L_1)), (\Delta V) = (\Delta L) / (\Delta T), (V) = ((V_2) - (V_1)).$$

Where (ΔT) is the difference in time between arbitrary tow points 1 and 2, also (ΔL) is the difference in distances between the same arbitrary tow points 1 and 2. The rip current velocities for magnitude and direction due to the combination of waves and currents in the presence of a deflector with angle (ϕ) calculated using, (Sine and Cosine) theories.

$$\frac{(\sin(A))}{a} = \frac{(\sin(B))}{b} = \frac{(\sin(C))}{c} \quad (13)$$

$$b^2 = a^2 + c^2 - 2a.c(\cos(B)) \quad (14)$$

Where: (A) is the angle between the rip current vector component and the resultant velocity due to the combination of wave and rip current, (B) is the angle of the deflector (ϕ), and (C) is the angle between wave direction and the resultant velocity due to the combination of wave and rip current. In equations (13) and (14), the magnitude of the wave, rip current, and the resultant combination between each other are a, c, and b, respectively. The percentages of rip current deflection due to the presence of deflectors in the path of the rip neck are 50%, 29.3%, and 13.4% for deflector angles 60, 45, and 30 degrees, but for case (A), the percentage of rip current deflection is zero. For different frequencies, 15, 20, 25, 30, 35, and 40 cycles/minutes, as shown in figures from (9 to 14). The measured velocities are 11.20, 10.11, 7.90, 6.24, 5.20, and 3.83 cm/sec; for case (A), there is no deflector. For case (B) deflector at a distance of 95 cm, the measured velocities are 14.20, 12.17, 9.70, 11.88, 7.34, and 10.50 cm/sec. For case (C) deflector at a distance of 105 cm, the measured velocities are 13.90, 13.61, 10.50, 8.23, 7.35, and 8.08 cm/sec. For case (D) deflector at a distance of 125 cm, the measured velocities are 12.00, 11.19, 9.05, 7.24, 4.32, and 6.25 cm/sec., respectively.

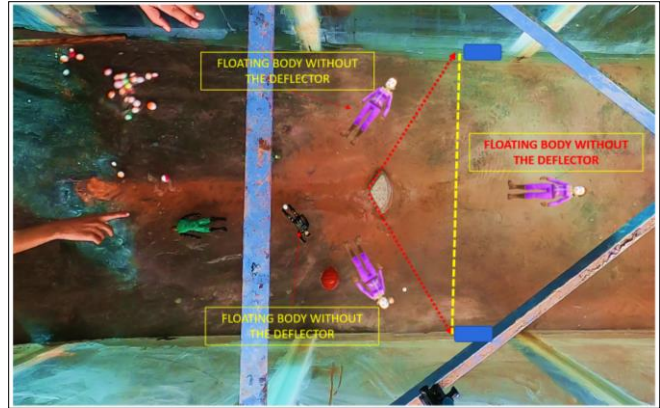


Fig. 9 The projected plan view shows the actual deflection of floating materials and subjects due to the presence of concrete deflectors; the experimental works are showing the actual behavior of floating subjects according to the different designed angles of the proposed deflector at different points and directions in the presence and the absence of deflectors.

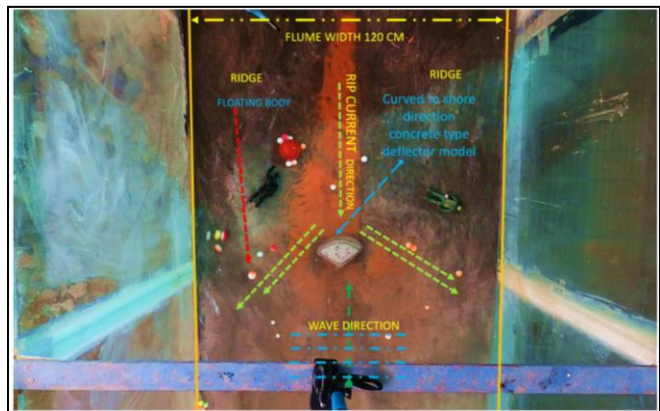


Fig. 10 The projected plan view shows the actual deflection of floating materials and subjects due to the presence of another type of concrete deflector. The experimental work shows the curved to shore concrete type of the proposed deflector and rib current deflected components.

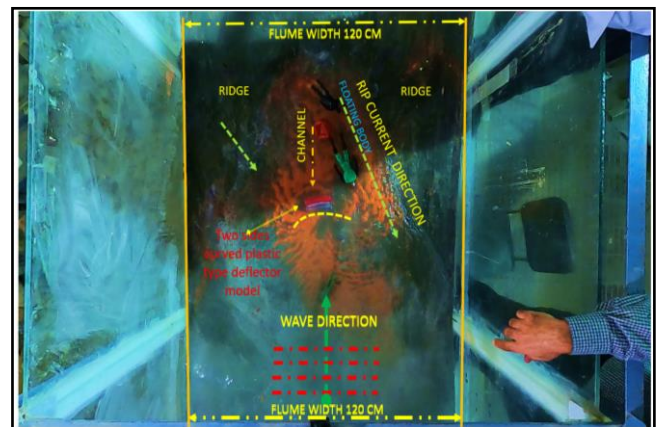


Fig. 11 The projected plan view shows the actual deflection of floating materials and subjects due to the presence of another type of plastic deflector. The experimental work shows the curved to shore plastic type of the proposed deflector and rib current deflected components.

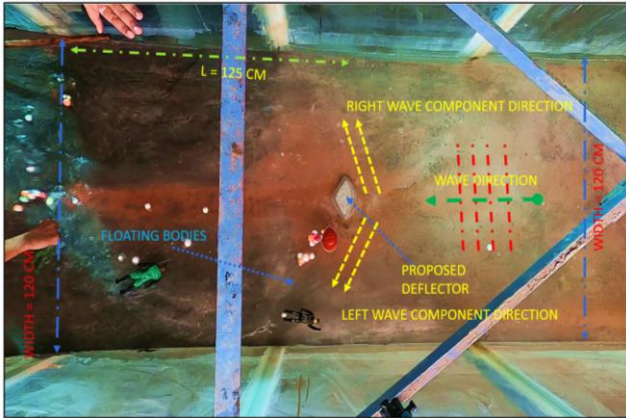


Fig. 12 The projected plan view shows the actual deflection of floating materials and subjects due to the presence of another type of concrete deflectors; the experimental work shows the curved to sea concrete type of the proposed deflector, left, and right wave-deflected components.

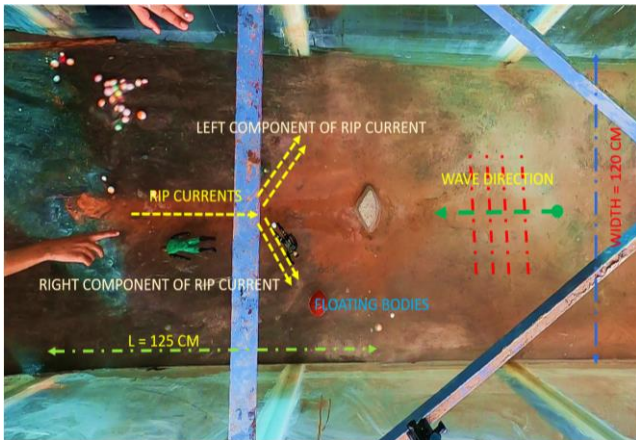


Fig. 13 The projected plan view shows the actual deflection of floating materials and subjects due to the presence of concrete deflector type; the experimental work shows the curved to sea concrete type of the proposed deflector and rib current deflected left and right components.

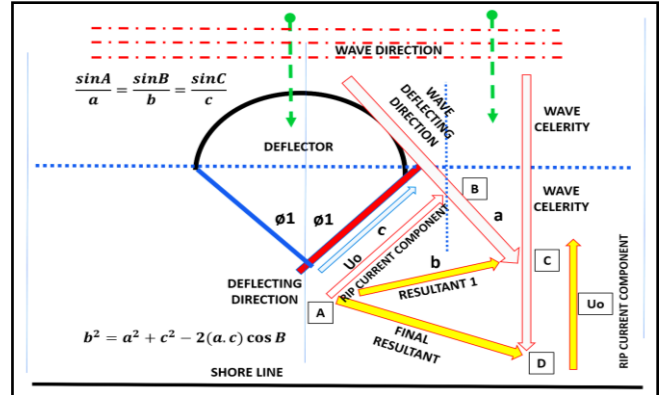


Fig. 14 The sketch shows the projected plan of the tangential wave component with thick red arrows, the cross-shore component of the wave, and the rip current component. Due to the combination of waves and currents in the presence of a deflector with a designed angle (ϕ_1). The rip currents deflected two times, one from the effects of the deflector and the tangential wave component resulting in a new component (Resultant 1) and the second deflection was due to the cross-shore component of the wave getting the final resultant.

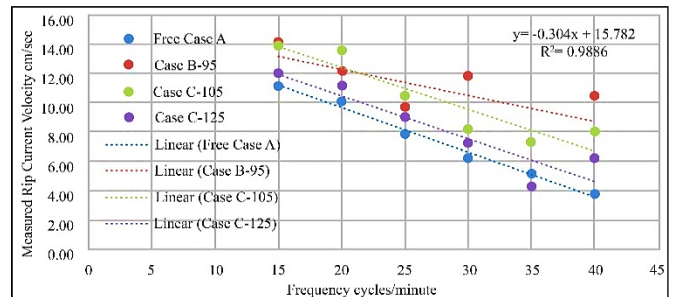


Fig. 15 The values of measured velocities for different locations of the proposed deflector, distances were 0.00 m for reference case A, 95.00 m for case B, 105.00 m for case C, and 125.00 m for case D, the significant wave heights were measured and calculated using measuring devices of wave height according to the frequencies from 20 cycle/min. to 40 cycles/min. The distances were measured in centimeters and time in seconds.

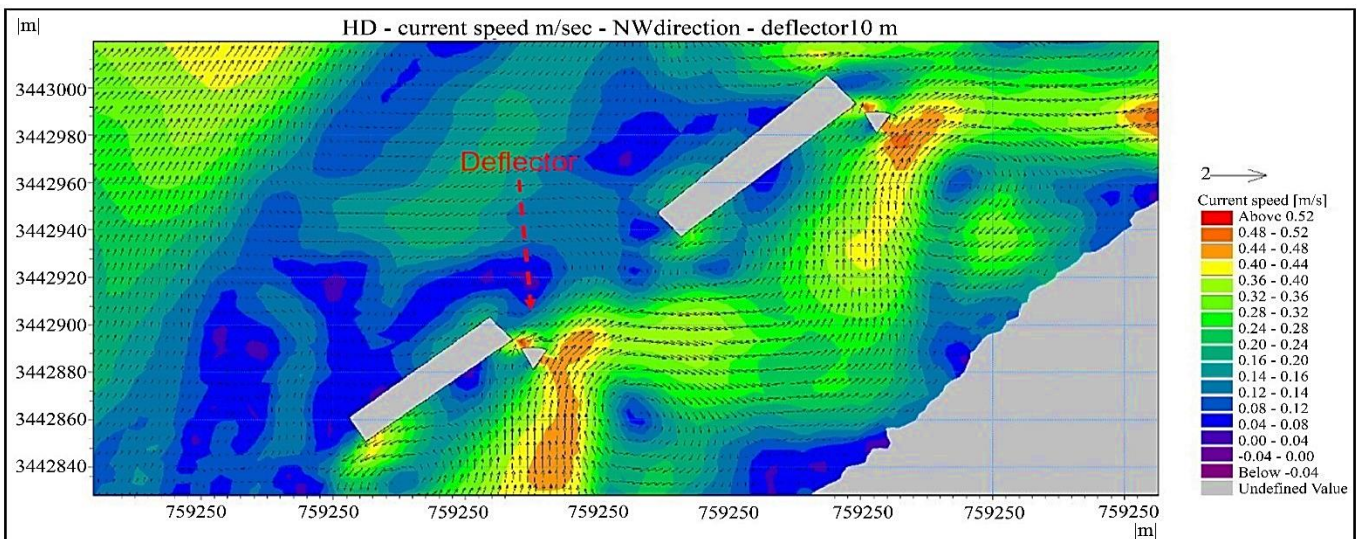


Fig. 16 The rip current velocities at detached breakwaters using a deflector at the Egyptian north coastal zone between longitudes $29^{\circ} 43' E$ and $29^{\circ} 42' E$ and latitude $31^{\circ} 6' N$. In the study area, the wave direction was chosen Northwest, according to the real data of the dominant direction of waves near the shoreline.

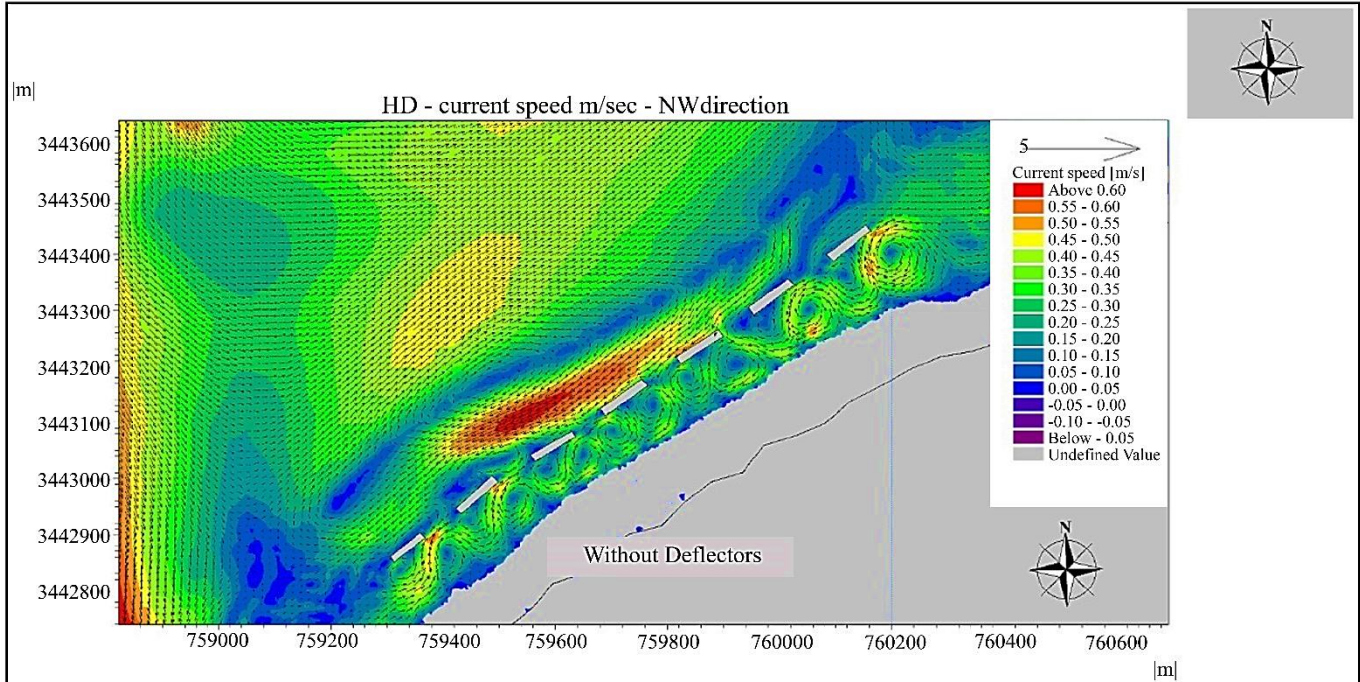


Fig. 17 The rip current velocities at detached breakwaters without deflectors at the Egyptian north coastal zone between longitudes 29° 43' E and 29° 42' E and latitude 31° 6' N. In the study area, the wave direction was chosen Northwest, according to the real data of the dominant direction of waves near the shoreline.

4. Result and Discussion

This present study presents a vision for the decision-makers by using a new technique to redirect and control the rip currents. The experiments were carried out as mentioned before using different locations for the deflectors at distances (125cm, 105cm, 95cm, and 0.00 cm) from the shoreline, different frequencies (20 rpm, 25 rpm, 30 rpm, 35 rpm, and 40 rpm), and different water depths of 7.5 cm, 10 cm, and 15 cm. As well as different forms of deflectors using concrete and perforated plastic materials. The concrete-type deflector has two forms, one curved towards the beach and the second towards the sea; also, the perforated plastic-type deflector has two forms, one curved towards the beach and the second towards the seaside. The analysis of the measured experimental data, using the experimental reference case (A) (the proposed deflector doesn't exist) and by the distribution of fluorescent sand tracers, tiny floating foam pieces, and very small colored pieces from papers along the surface area of the water during the experiments showed that the formation of feeding currents parallel to the shoreline and rip currents perpendicular to it. These rip currents differed in their values and directions, depending on the changes in the characteristics of the incoming waves to the experimental beach and the characteristics of the experimental beach itself. It is observed that the speed of experimental floating small objects in the rip area decreased as the body approached the head area of rip currents. Also, the directions of the experimental floating objects changed from zero to 90 degrees clockwise or anticlockwise according to the position of the objects, then from 90 to 180 degrees, and they returned

to the experimental shore. The experimental floating objects returned to the shoreline as a result of the vanishing of the rip current surface velocity, in addition to the effect of the consequent incoming waves in the direction opposite to the rip current direction. This was the reason which made the floating objects return in the direction opposite to the main rip current direction. After analyzing data of the experiments from the experimental cases (B, C, and D). The results showed that the rip currents were deflected due to the effect of placing the proposed deflector, a type of concrete with a curved face towards the sea, in the path of the rip current at a distance of 125 cm from the shoreline and their directions became parallel to the angle of inclination of the deflector. Also, when changing the place of the proposed deflector from 125 cm to 105 cm and 95 cm from the shoreline, the rip currents were deflected, and their directions became parallel to the angle of inclination of the deflector. Repeating the experiments using the second type of the proposed deflector of a type of concrete with a curved face towards the shore, the results showed that the rip currents were deflected. Their directions became parallel to the angle of inclination of the deflector, but with the presence of erosion at its corners, with the rise of the water level at a stagnation point in the frontal mid part of the deflector. Repeating the experiments using the perforated plastic type, curved from both sides towards the sea and towards the shore. It is observed that the effects of the deflector on directing the rip current and on directing floating objects exist, but the rip current direction, resulting from the deflector, was tangent to the curved part of the deflector. The presence of eddies and scour of the bed when

using these types of deflectors were also seen. The same results were obtained for different distances at 125 cm, 105 cm, and 95 cm from the shoreline. The percentages of rip current deflection due to the presence of deflectors in the path of the rip neck were (50%, 29.3%, and 13.4%) for deflector angles (60, 45, and 30 degrees). Still, for case (A), the percentages of rip current deflection were zeros for the same frequencies (15, 20, 25, 30, 35, and 40 cycles/minutes), as shown in figure (15). The comparison between measured velocities in case (A) and the other cases (B, C, and D) showed increasing in rip current speeds, not in rip current directions, the clarification that the experimental flume cross-section was constant because it had a fixed width, so for the same water depth, the water discharge passing through it was constant according to continuity principal. The deflector had average width equal to the width of the rip channel. Hence, the presence of a deflector in the present experimental rip channel reduced the cross-section of its rip channel, so the velocity increased in its speed due to the reduction of the cross-sectional area of the rib bed channel. The field conditions at beaches and rip currents differ from the flume conditions, so using prototypes for the proposed deflectors is recommended. This research's main goals are assessing the proposed deflector to deflect the rip currents and assessing the horizontal designed angle (θ) in directing the floating bodies. The experiments showed different values of rip current deflections due to the presence of deflectors. So applying the MIKE 21 module for two different scenarios as shown in figures (16 and 17), whereas the first scenario was the keeping of the existing detached breakwater without deflectors; for the case of waves in the Northwest (NW) direction, rip currents were formed in the North-East direction with values from (0.45 to 0.60) m/s; and angle about (10) degrees with north direction. The second scenario was the existence of deflectors in the path of rip currents; for the case of waves in the Northwest (NW) direction, rip currents were formed in the North-East direction with values from (0.20 to 0.45) m/s and angle (88) degrees with north direction. comparing the results of the two different scenarios showed that, with a reduction in velocity values from 25% to 55%, the deflectors directed the currents by (78) degrees from the reference case without deflectors, so the directed currents can help the floating swimmers to escape from rip currents in the direction parallel to the shore. The comparison between measured velocities concerning distances for different frequencies in case (A) and the other cases (B, C, and D) showed that the distance of the deflector from the shoreline has an important effect on rip current velocities. The big the measured distance, the less measured velocity, and then the measured distances of the deflector from the shoreline are inversely proportional to rip current velocities. The study's results showed that the proposed systems could reflect about 13.4% to 50% of the rip currents depending on the deflector type and angles. For case (B), the measured

velocities were 14.20, 12.17, 9.70, 11.88, 7.34, and 10.50 cm/sec. For case (C), the measured velocities were 13.90, 13.61, 10.50, 8.23, 7.35, and 8.08 cm/sec. For case (D), the measured velocities were 12.00, 11.19, 9.05, 7.24, 4.32, and 6.25 cm/sec., respectively.

5. Conclusion

From the previous discussion, it is concluded that the best type of the proposed device is the concrete type with a curved face to the sea; it is also concluded that the deflector frontal curved part converts coming waves into tangential waves. The tangential coming waves interact with the directed rip currents. As a result of this combination creates a new resultant rip current (streamline) with some value and direction that depends on the directed currents and the tangential waves. From the previous analysis, it is concluded that the proposed deflector is controlling the values and directions of the rip currents with a reduction in velocity values from 25% to 55%, preventing floating objects from moving toward the sea or moving with the rip currents, which leads to an increase in the probability of surviving drowning due to rip currents. It is concluded that the angle of the deflector (θ) plays an important role in the deflection percentage of rip currents, consequently deflecting the floating subjects caught by rip currents. Also, it is concluded that the angle of inclination of the sides of the proposed deflector greatly affects the direction of the rip currents. The deflector also directs the rip current to sea direction with a tilted angle nearly parallel to shore. It is concluded that the effect of the deflector in the neck rip area is greater than its effect in the head area of the rip current. Also, it is noticed that the position of the deflector is very effective when the waves have high frequencies, while the effect of the deflector on rip currents decreases at great depths of water. Also, this study concludes that the use of deflectors can mitigate drowning effects and increase the preservation of lives. Finally, for decision-makers, the proposed deflector should be checked and modified using prototypes in the field conditions. After that, it can be used as a new tool to deflect rip currents to save lives. So the angle of the deflector (θ) plays an important role in the deflection percentage of rip currents, consequently deflecting the floating subjects caught by rip currents. The distance of the deflector from the shoreline has an important effect on rip current velocities.

Data availability

The datasets used and/or analyzed during the current study are available from the corresponding author upon reasonable request.

Ethical approval

This article does not contain any studies with human participants or animals performed by any authors.

References

- [1] Bader A.A, and Shatta M.M., “The Effects of Baltim Detached Breakwaters on the Grain Size Variations and Littoral Sand Drift, Egypt,” *Bulletin of the National Institute of Oceanography and Fisheries*, A.R.E, 2002
- [2] B. Chris Brewster, Richard E. Gould, and Robert W. Brander, “Estimations of Rip Current Rescues and Drowning in the United States,” *Natural Hazards and Earth System Sciences*, vol. 19, pp. 389–397, 2019.
- [3] CAPMAS the Central Agency for Public Mobilization and Statistics Egypt, A Report Issued, 2018.
- [4] Shari L.Gallop et al., “Perceptions of Rip Current Myths from the Central South Coast of England,” *Ocean & Coastal Management*, vol. 119, pp. 14-20, 2016. *Crossref*, <https://doi.org/10.1016/j.ocecoaman.2015.09.010>
- [5] Robert A. Dalrymple, "Rip Currents and Their Causes," *Journal of Coastal Engineering*, no. 16, 1978. *Crossref*, <https://doi.org/10.9753/icce.v16.83>
- [6] Earl Sinchuk, Marquette, and Michael Rosinsky, “*Rip Current Sensor and Warning System with Anchor*,” United States, Patent Application Publication, 2013.
- [7] Elmooty M.A, Taha, S.E, "Rip Current Causes and Precautions," *Proceeding of the 9th International Conference*, 2012.
- [8] Victor A. Gensini, and Walker S. Ashley, "An Examination of Rip Current Fatalities in the United States Natural Hazards, vol. 54, pp. 159-175, 2009. *Crossref*, <https://doi.org/10.1007/s11069-009-9458-0>
- [9] Kevin A. Haas et al., “Quasi-Three-Dimensional Modeling of Rip Current Systems,” *Journal of Geophysical Research*, vol. 108, no. C7, 2003. *Crossref*, <https://doi.org/10.1029/2002JC001355>
- [10] Merrick C Halle, "*Rip Current Dynamics and Nearshore Circulation*," Doctor Philosophy in Civil Engineering, Faculty of Engineering the University of Delaware, 1999.
- [11] Herrington, “*Rip Currents: Nearshore Fundamentals*,” Ocean Lecture & Educator’s Night, University Corporation for Atmospheric Research, COMET Modules, 2012.
- [12] MM Iskander et al., “Overpopulation and Rip Current Mitigation Plan for the Egyptian Coasts,” *Ministry of Water Resources & Irrigation Cairo Water Week, CWW2021-Proceeding*, Cairo, Egypt, pp. 24-28, 2021.
- [13] Kim Nam-hoon et al., “*Disaster Prevention and Alarm System for Rip Current*,” Introduced Patent no. KR20120069253A in South Korea, 2012.
- [14] “*Buoy for Detecting Rip Current*,” Introduced Patent no. KR101221688B1 in South Korea, 2013.
- [15] Jamie MacMahan et al., "An Introduction to Rip Currents Based on Field Observations," *Journal of Coastal Research*, West Palm Beach, Florida, vol. 27, no. 4, 2011. *Crossref*, <https://doi.org/10.2112/JCOASTRES-D-11-00024.1>
- [16] Andrew Morang, Joann Mossa, and Robert J. Larson L, "*Technologies for Assessing the Geologic and Geomorphic History of Coasts*," Chapter 3 Field Data Collection and Observation of Us Army Corps of Engineers, 1993.
- [17] Neil John Wallace, Port Ma Quarry, Australia, US Patent No. 9,180,937 B2, 2015.
- [18] Reda M. A. Hassan, and Shaymaa E.T. Hassan, “Alleviation of Deadly Hazards of Rip and Circulation Currents Using Near Shore Self Lighting Floating Units,” *Journal of American Science*, Marsland Press, vol. 15, no. 12, pp. 28-38, 2019.
- [19] Svendsen, I. A., K. Haas, and Q. Zhao, “*Quasi-3D Nearshore Circulation Model*,” Technical Report of Center for Applied Coastal Research, University of Delaware, Newark, DE, p. 15, 2003.
- [20] G.Harikrishnan, and Seethalakshmi.S, "Appearance of Midair plasma extenuation of Shock Wave," *SSRG International Journal of Applied Physics*, vol. 3, no. 1, pp. 18-22, 2016. *Crossref*, <https://doi.org/10.14445/23500301/IJAP-V3I2P104>
- [21] Taha. S, “*The Hydraulic Analysis of the Circulations and Rip Currents*,” Thesis of Master in Sc. Hydraulics and Irrigation Engineering, Faculty of Engineering, Alexandria University, 2016.
- [22] Thomas J. Lochtefeld, “Method and Apparatus for Controlling Break Points and Reducing Rip Currents in Wave Pools,” Introduced the Patent No. US6738992B2 in the United States, 2004.
- [23] T. S. Hedges, “Combinations of Waves and Currents: An Introduction,” *Proceedings of the Institution of Civil Engineers*, vol. 82, no. 3, pp. 567-585, 1989. *Crossref*, <https://doi.org/10.1680/iicep.1987.319>
- [24] H.J.De Vriend, and M.J.F.Stive, “Quasi_3D Modeling of Nearshore Currents,” *Coastal Engineering*, vol. 11, no. 5-6, pp. 565-601, 1987. *Crossref*, [https://doi.org/10.1016/0378-3839\(87\)90027-5](https://doi.org/10.1016/0378-3839(87)90027-5)
- [25] G Winter, "*Rip Current Characteristics at the Dutch Coast Egmondaan Zee*," Master of Science in the field of Civil Engineering at Delft University of Technology Delft, The Netherlands, 2012.
- [26] Tae-Myoung Oh, and Robert G. Dean, “Three Dimensional Hydrodynamics on Barred Beach,” *Coastal Engineering Proceedings*, 1996. *Crossref*, <https://doi.org/10.9753/icce.v25.%25p>